Nuclear Instruments and Methods in Physics Research A 1057 (2023) 168686

Contents lists available at ScienceDirect

Nuclear Inst. and Methods in Physics Research, A

journal homepage: www.elsevier.com/locate/nima

Qualification of the X-ray spectral performance of the DEPFET pixels of the DSSC imager

A. Castoldi [a,b,*], M. Ghisetti [a], C. Guazzoni [a,b], S. Aschauer [c], L. Strüder [c], K. Hansen [d], S. Maffessanti [d], C. Danilevski [e], D. Lomidze [e], M. Turcato [e], M. Porro [e,f]

[a] Politecnico di Milano, Dip. Elettronica, Informazione e Bioingegneria, 20133, Milano, Italy
[b] Istituto Nazionale di Fisica Nucleare, Sez. Milano, 20133, Milano, Italy
[c] PNSensor GmbH, 81739, Munich, Germany
[d] Deutsches Elektronen-Synchrotron DESY, 22607, Hamburg, Germany
[e] European XFEL, 22869, Schenefeld, Germany
[f] Universita' Ca' Foscari Venezia, Dipartimento di Scienze Molecolari e Nanosistemi, 30172 Venezia, Italy

A B S T R A C T

The first DEPFET module (128 x 512 pixels) of the DSSC pixel detector, designed for user experiments at the European XFEL, has been fully instrumented and an experimental campaign has been carried out with X-ray lines to qualify the main performance figures and to collect calibration data. X-ray spectra fitting has been optimized with consideration to the main sources of systematic errors to achieve gain calibration within 1% accuracy, which is a key issue for its successful operation at the European XFEL. The most important result is the equivalent noise charge of 16 el rms on average. This shows the potential of the DEPFET-based pixel to reach single-photon imaging down to the lowest photon energy (0.25 keV) at 4.5 MHz frame frequency that can be extrapolated at camera level with high confidence.

1. Introduction

The DEPFET Sensor with Signal Compression (DSSC) [1] is a 1 Mpixel X-ray hybrid pixel detector designed for user experiments at the European XFEL [2]. The main requirements for 2D X-ray imaging detectors posed by the unique combination of brilliance and time structure of the European XFEL bunch scheme are the maximum frame frequency of 4.5 MHz, the dynamic range up to 10^4 and photon counting capability in the photon energy range of interest. The DSSC camera, in particular, is targeted to the low-energy range, i.e. between 0.25 keV and 6 keV, which adds further demanding requirements on the noise performance and on the entrance window. A first camera was completed and commissioned at the SCS beam line in 2019. It is based on hexagonal pixels with a passive anode, readout by the linear spectroscopic chain on the ASIC. It achieved an electronic noise level of about 60 electrons rms on average at the fastest readout speed (4.5 MHz frame rate, 50 ns filter integration time) and a maximum dynamic range of 9 bit (at frame rates $<$4.5 MHz).

In order to provide the necessary improvement in noise and dynamic range, a second detector is under development featuring DEPFET-based readout of the pixels. The concept of the standard DEPFET was adapted to the DSSC project in order to add signal compression at sensor level, with the goal to extend the dynamic range while preserving the low noise performance that DEPFETs can provide thanks to the very low input capacitance [3]. The fabrication process of the sensor is based on a commercial high-voltage 0.35 μm CMOS process for the DEPFET side and a custom process for the realization of the back side (entrance window) [4]. The readout ASIC is the same as for the first camera, the analog section having a second branch designed for DEPFET readout. The potential features of this detector are therefore quite unique in the landscape of several X-ray imaging detectors currently under development, see for instance [5–8].

The first DEPFET module (128 x 512 pixels) has been fully instrumented and an experimental campaign has been carried out with X-ray lines to qualify the main performance figures and to collect high-quality calibration data. The focus of this paper is on the qualification of the spectral performance of the DEPFET pixels and on the accurate extraction of gain and noise from the acquired X-ray spectra. The accuracy in the calibration of the DSSC camera *a priori* is, in fact, a key issue for its successful operation at the European XFEL. Given the limited ADC resolution, in order to provide single-photon sensitivity and the required dynamic range, the gain of the individual pixel channels must be trimmed to 1 photon energy per ADC bin (or an integer no. of bins) using the fine granularity of the available settings (about 1% for gain, about 0.1

* Corresponding author. Politecnico di Milano, Dip. Elettronica, Informazione e Bioingegneria, 20133, Milano, Italy.
E-mail address: Andrea.Castoldi@polimi.it (A. Castoldi).

https://doi.org/10.1016/j.nima.2023.168686
Received 15 May 2023; Accepted 12 September 2023
Available online 15 September 2023

ADU for offset). Therefore pixel calibration data with comparable accuracy is needed to configure the detector before the experiment [9,10]. As the available X-ray energies at the beam line are not ideal for this task (e.g. < 3 keV at the SCS and SQS beam lines at the European XFEL), we conducted a separate experimental campaign using a pulsed X-ray source providing higher-energy lines to collect the first high quality calibration data of the novel DEPFET module. Moreover, the measured noise of the first DEPFET module, which is the smallest independent unit, is considered representative of the spectral performance of the future 1 Mpixel camera (i.e. 16 modules).

The paper will summarize and critically discuss methods and experimental results. Section 2 describes the experimental setup of the DEPFET module and of the pulsed X-ray source. Section 3 discusses the methods used to extract gain and noise from the X-ray spectra and the major sources of systematic errors. Section 4 presents and discusses the relevant results and the distribution of gain and noise over the module. Section 5 includes conclusions and the outlook of the next steps.

2. Experimental setup

The heart of the DEPFET module (or ladder) is made of two 725 μm thick monolithic sensors (each 128 x 256 pixels) bump-bonded to 16 ASICs (64x64 pixels). Fig. 1 shows the layout of individual pixels and of the full ladder. The hexagonal pixel shape (136 μm side length, equivalent to a square pixel of 219 μm side), was chosen to mitigate charge sharing effects. The DEPFET is located in the centre and 2 p+ drift rings favour charge collection and minimize crosstalk. The experimental setup was mounted in the clean room of the European XFEL Detector group where the DEPFET module has been instrumented inside the FENICE vacuum vessel, mechanically coupled to a cooling copper block connected to an external cryopump to provide stable operating conditions. For this first experimental campaign we set the temperature of the focal plane at T = 18 °C. FENICE vessel provides an entrance window mounted on a CF160 flange that allows irradiation of the full sensitive area of the DEPFET ladder.

The pulsed X-ray source (PulXar [11]) is based on an electron gun and fast deflection plates before the electron bunch hits the anode target, allowing generation of X-ray pulses as short as 30 ns and trains of several hundred pulses with burst frequency up the highest value used at the European XFEL (4.5 MHz).

Although the number of photons per pulse is obviously lower than the European XFEL beam, PulXar source can reproduce the exact time structure of the X-ray pulses and, therefore, allows acquisition of calibration data in the same operating conditions of the European XFEL beamlines. For this first commissioning test of the DEPFET module at the European XFEL, we chose to limit the high voltage of the X-ray source to 25 kV, to minimize any chance of accidental radiation damage to the surface where DEPFETs are fabricated, and we used Cu anode target. Therefore we could still efficiently excite Cu X-ray fluorescence K lines, hard enough to obtain accurate calibration data. Beam filtration with a 50 μm thick aluminium (Al) sheet was added to suppress most of bremsstrahlung radiation below the Cu Ka (8.04 keV) peak, which is relevant for gain analysis. Due the exit pupil of PulXar, FENICE vessel was connected to PulXar by means of a 2 m long vacuum pipe, with sections of increasing diameter, to achieve irradiation of the full ladder area (about 52 mm × 120 mm). The whole setup is shown in Fig. 2.

For the experimental qualification of the DEPFET pixels, PulXar was configured to deliver 600 pulses, each of 30 ns duration, at the repetition frequency of 2.25 MHz. The DEPFET ladder was readout at 2.25 MHz, with filter integration time of 50 ns, filter flat top of 100 ns and a clear pulse of 100 ns to remove the signal charge from the DEPFET internal gate. Though the first tests were carried out at 2.25 MHz, the short integration time (50 ns) used is compatible with the fastest readout cycle at 4.5 MHz. Synchronization of PulXar pulses with DEPFET readout cycle is done by a preliminary delay scan, searching for the maximum amplitude that corresponds to pulse arrival inside the measuring window (100 ns filter flat top). The gain settings of the DEPFET ladder were configured "flat" on all the pixel (no gain trimming) with the highest gain of the filter and DEPFET drain current for all pixels was set to the nominal value (100 μA).

3. Analysis of the X-ray spectra

The acquired X-ray spectra were analyzed to extract gain, offset and noise for each pixel from the fitting results of the pedestal peak and of the Cu Ka line. Fig. 3 shows a typical single-pixel spectrum acquired with the DEPFET ladder in the experimental conditions described in Section 2. The fitting model of the X-ray spectra has been optimized to reduce systematic errors that eventually impact on the accuracy of the calibration dataset. The major effects to be considered are discussed in the following.

The Cu Ka line has an asymmetric shape due to the non-negligible fraction of partial events (i.e. charge sharing among neighbouring pixels and signal charges not completely collected within the time measuring window) which produce a continuum between the pedestal peak and the Cu Ka line. If the fitting model does not include an adequate description of this asymmetry, the resulting Ka centroid position would be inevitably shifted towards the pedestal, with direct impact on gain.

The main effect on the pedestal peak, instead, is due to low-resolution data binning. Due to the low-noise level achievable with DEPFET-pixels and the typical reference gain of 1 photon/ADU, the pedestal peak is often spread on very few bins and the rms width of the

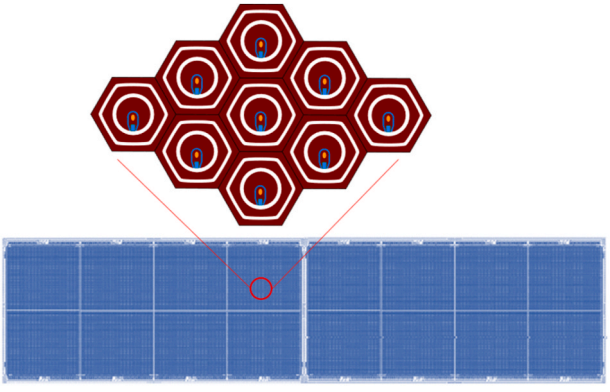

Fig. 1. Layout of the 128 x 512 pixel DEPFET ladder and of the hexagonal pixels.

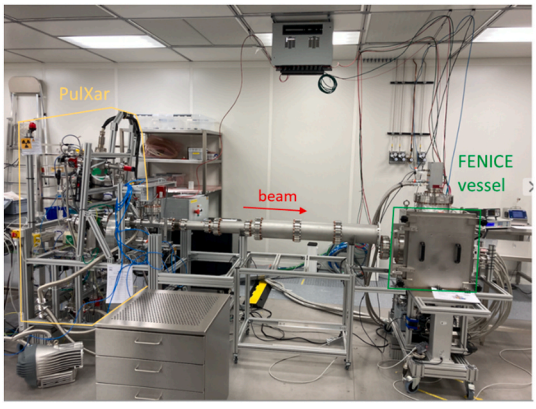

Fig. 2. Photograph of the experimental setup in the clean room (DET group, European XFEL). The 2 m long vacuum pipe connecting PulXar source and FENICE vessel (where the DEPFET ladder is instrumented) is visible in the centre.

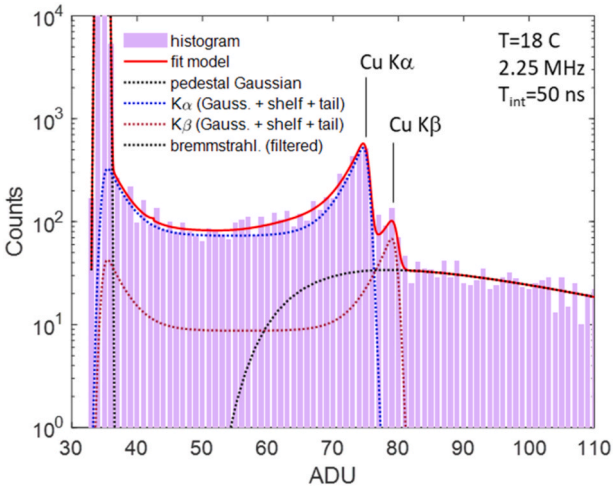

Fig. 3. Single-pixel spectrum of a DEPFET pixel with PulXar (25 kV, Cu target, Al 50 μm filter) at T = 18 °C. The global fit model (red) and the main spectral components are shown (dotted lines). For each spectral line, a flat term ("shelf") and an exponential decaying term ("tail") are included to describe the incomplete collection effects. A small contribution of bremsstrahlung under the Ka and Kb peaks is visible.

peak is well below one ADU (i.e. <0.3 ADU in the presented case). Therefore, fitting with a standard Gaussian function would lead to a systematic overestimate of the sigma (error depending on the position of the peak with respect to the ADC bin edges). This issue can be effectively minimized by bin integration of fit errors. As an example, from the analysis of dark spectra it was shown in [12] that fitting the pedestal peak with a standard Gaussian fit gave sigma values of 0.341 ADU ± 0.07 ADU (mean ± standard deviation over the ladder) resulting in a discrepancy of about 40% on the estimate of noise performance with respect to a bin-integrated Gaussian (0.243 ADU ± 0.07 ADU) which closely matches the expected noise distribution.

To mitigate the impact of the low-resolution in-pixel ADC (8–9 bit) it is needed to tailor the fitting model of the low-energy continuum specifically to the DEPFET pixel detector, which was carried out in previous works with high resolution external readout [13]. It should be remarked that the ADC differential nonlinearity (DNL) is not negligible and can be qualitatively appreciated in Fig. 3, e.g. in the plateau between pedestal and Ka peaks. For the purpose of producing calibration data from reference lines, the use of a hard X-ray line (as in this case) is generally sufficient to mitigate the impact of DNL. However correction techniques of the DNL errors should be investigated to improve performance of the DEPFET pixels in the foreseen experiments at the European XFEL with low energy photons.

Fig. 4 shows the distribution of gain and of the root mean square error (RMSE) of the fit of the Cu Ka peak, for different fitting models considered, to estimate the impact of increasing number of peak-shape components. The peak shape functions were derived from [14]. Fitting the Cu Ka peak with a single Gaussian term, in fact, gives the distribution with smallest gain values, visible in Fig. 4 (left). By adding progressively more peak-shape details ("shelf" and exponential "tail" for each X-ray line) and the bremsstrahlung background (Kramer's law), the gain distribution shifts to the right, as expected. The beneficial impact of the increased accuracy of the fitting model is also confirmed in Fig. 4 (right) where the RMSE is progressively reduced. Bin integration has been added on the complete model showing negligible impact on peak centroid positions and therefore on gain (while the significant effect is on pedestal sigma, as mentioned above). The fit function with the more complete model used in this paper is shown in Fig. 3 (red line) together with its spectral components (dotted lines).

4. Results and discussion

As it is returned by the fitting function, bremsstrahlung intensity is also available for analysis. As the counts beyond the Cu K lines are mostly due to bremsstrahlung, the estimate is in general quite precise (few percent). Fig. 5 shows the map over the full ladder of the bremsstrahlung intensity which is a useful monitor of the beam intensity profile on the detector, in this case not perfectly centred. The reduction of charge collection efficiency in proximity of the two edges of the sensors is also visible.

The distribution of the gain over the ladder is shown in Fig. 6. The map shows the pattern of the 16 ASICs with the dispersion of the gain for the nominal setting (no gain trimming was performed). Looking in detail, a band of about 10 rows both at the top edge and at the bottom edge of the ladder shows a more homogeneous distribution. This is better revealed by comparing the histograms of the first 10 rows (5120 pixels) to the total. The gain spread of 3.5% over the full ladder, already rather small, drops to about 1.6% in the edge regions. The accuracy of gain estimation can be verified composing the standard error of the two

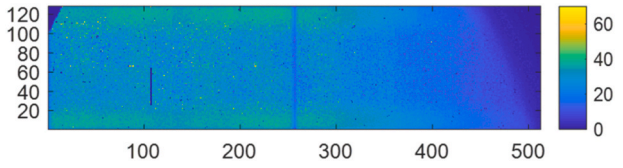

Fig. 5. Bremsstrahlung intensity recorded by the DEPFET ladder coupled to PulXar.

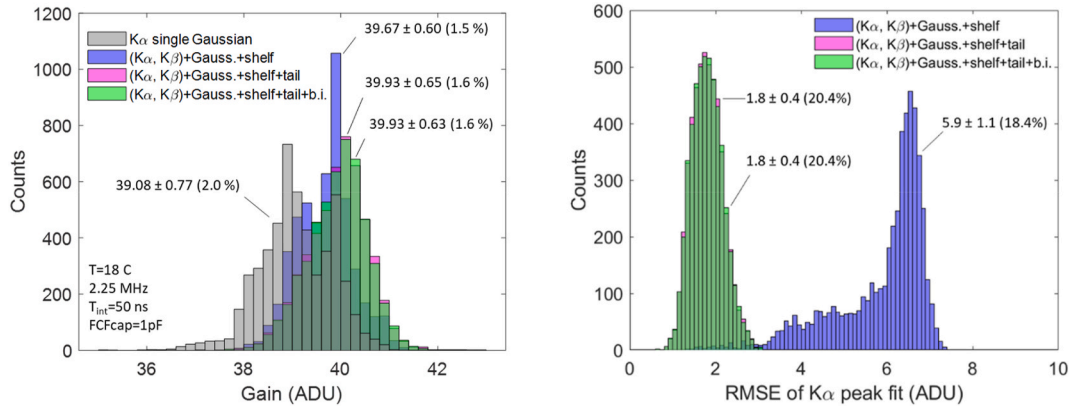

Fig. 4. Histograms of gain (distance between pedestal and Cu Ka peak) (left) and of the root-mean-square error of the fit of the Ka peak (right) for different fitting models of the Cu K lines. Pixels of rows 0–9 are considered to minimize impact of DNL errors. The mean and standard deviation are given.

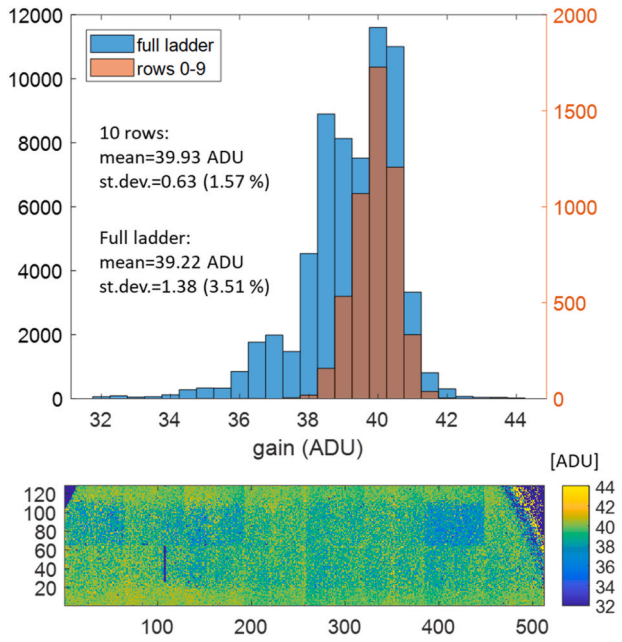

Fig. 6. Results of gain calibration on the DEPFET ladder. (Top) Histogram of gain (distance between pedestal and Ka peak) of the whole ladder (blue bars, left vertical axis) and of the first 10 rows (red bars, right vertical axis). (Bottom) Map of gain over the ladder. The two bands near the top and bottom edge with better homogeneity are visible.

peak centroids which turns out to be 1% or less (rows 0–9), which is satisfactory.

It is interesting to correlate the extracted gain values and the intensity profile of the incident beam. To this purpose Fig. 7 shows the 1-D profile of the bremsstrahlung intensity along the horizontal axis and of the corresponding values of the gain (average of rows 0–4). Bremsstrahlung intensity in the right sensor clearly shows the decrease as it enters the region of penumbra, practically dropping to zero at the right edge. Despite the large intensity variation, gain does not appear to change appreciably, which confirms the reliability of the fitting procedure.

The equivalent noise charge (ENC) is shown in Fig. 8. From the map we see again the more homogeneous distribution in the top and bottom edge regions, as observed in the gain map. The pattern of the edge rows versus the internal rows can be correlated to the values of the DNL error, which showed a similar pattern (higher DNL error in the central rows). This would explain the larger non-uniformity of the resulting gain and noise observed in the central rows. The achieved ENC is within 10–20 el rms over most of the ladder which confirms the expected noise performance of the DEPFET pixels. These results at ladder level can be extrapolated with a high confidence level to predict the noise performance of the DEPFET-based camera under development to be about a factor of 3 better than the first camera.

5. Conclusion and perspectives

The qualification of the spectral performance of the first DEPFET module (128 x 512 pixels) and the extraction of calibration data (gain and noise) from the acquired X-ray spectra has been carried out for the first time at the European XFEL. The procedure to calibrate the gain and to extract the noise level has been validated on X-ray spectra with Cu fluorescence lines to estimate the noise performance at ladder level and gain calibration with adequate accuracy.

The fitting procedure of X-ray spectra has been optimized and it is now well understood. The main sources of systematic errors have been minimized and the obtained gain values are considered to be within 1%

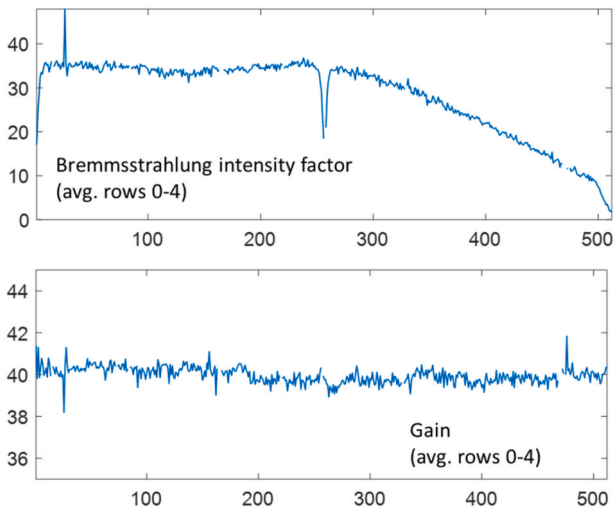

Fig. 7. 1-D profile of Bremsstrahlung intensity (top) and gain (bottom) along the horizontal direction. The first 5 rows (0–4) have been averaged to reduce random fluctuations. The drop of the detected intensity in the middle (top plot) corresponds to edge effects of the right and left sensors. No appreciable trend of the gain is visible despite the large variation of intensity due to the penumbra on the right sensor.

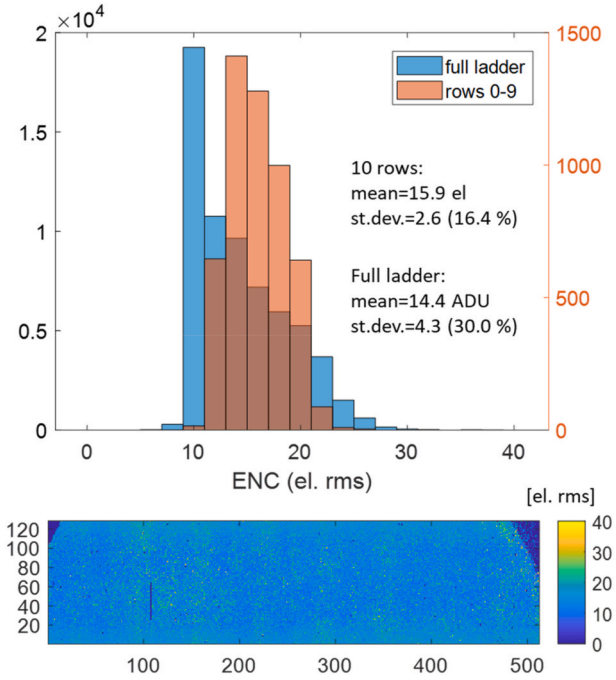

Fig. 8. Equivalent noise charge (ENC) extracted from the sigma of the Gaussian of the pedestal peak. (Top) Histogram of the ENC of the whole ladder (blue bars, left vertical axis) and of the first 10 rows (red bars, right vertical axis). (Bottom) Map of the ENC over the ladder. The two bands near the top and bottom edge with better homogeneity are visible.

accuracy. Further investigation of the impact of DNL errors and related correction techniques is also in progress.

The most important result is the equivalent noise charge of 16 el rms on average. It shows the potential of the DEPFET-based pixel to reach single-photon imaging down to the lowest photon energy (0.25 keV) at ladder level and therefore at camera level, as it is formed by 16 independent ladders. The optimization of the operating conditions, starting from temperature and filter integration time, will also be investigated as may further improve noise performance as far as sensor leakage and

thermal noise of the DEPFET channel are the dominant noise contributions.

Declaration of competing interest

The authors declare that they have no known competing financial interests or personal relationships that could have appeared to influence the work reported in this paper.

Acknowledgements

This work has been carried out in the framework of the DSSC project funded by the European XFEL GmbH.

References

[1] M. Porro, et al., The MiniSDD-based 1-Mpixel camera of the DSSC project for the European XFEL, IEEE Trans. Nucl. Sci. 68 (6) (June 2021) 1334–1350, https://doi.org/10.1109/TNS.2021.3076602.
[2] W. Decking, et al., A MHz-repetition-rate hard X-ray free-electron laser driven by a superconducting linear accelerator, Nature Photon. 14 (6) (2020) 391–397.
[3] G. Lutz, P. Lechner, M. Porro, L. Strüder, G. De Vita, DEPFET sensor with intrinsic signal compression developed for use at the XFEL free electron laser radiation source, Nucl. Instrum. Methods Phys. Res. A, Accel. Spectrom. Detect. Assoc. Equip. 624 (2) (Dec. 2010) 528–532.
[4] S. Aschauer, et al., First results on DEPFET active pixel sensors fabricated in a CMOS foundry—a promising approach for new detector development and scientific instrumentation, J. Instrum. 12 (11) (2017). Nov.
[5] G. Blaj, et al., X-ray detectors at the linac coherent light source, J. Synchrotron Radiat. 22 (3) (May 2015) 577–583, https://doi.org/10.1107/S1600577515005317.
[6] A. Mozzanica, et al., The JUNGFRAU detector for applications at synchrotron light sources and XFELs, Synchrotron Radiat. News 31 (6) (Nov. 2018) 16–20, https://doi.org/10.1080/08940886.2018.1528429.
[7] A. Marras, et al., Characterization of the Percival detector with soft X-rays, J. Synchrotron Radiat. 28 (1) (Jan 2021) 131–145, https://doi.org/10.1107/S1600577520013958.
[8] L. Strüder, et al., Large-format, high-speed, X-ray pnCCDs combined with electron and ion imaging spectrometers in a multipurpose chamber for experiments at 4th generation light sources, Nucl. Instrum. Methods Phys. Res. A, Accel. Spectrom. Detect. Assoc. Equip. 614 (3) (Mar. 2010) 483–496, https://doi.org/10.1016/j.nima.2009.12.053.
[9] G. Weidenspointner, S. Schlee, A. Castoldi, C. Guazzoni, S. Maffessanti, M. Porro, Study of systematic and statistical uncertainty in offset, noise, and gain determination of the DSSC detector for the European XFEL, in: 2017 IEEE Nuclear Science Symposium and Medical Imaging Conference, NSS/MIC), Atlanta, GA, USA, 2017, pp. 1–4, https://doi.org/10.1109/NSSMIC.2017.8532911.
[10] A. Castoldi, et al., Calibration strategy of the DSSC X-ray imager, in: 2019 IEEE Nuclear Science Symposium and Medical Imaging Conference, NSS/MIC), Manchester, UK, 2019, pp. 1–3, https://doi.org/10.1109/NSS/MIC42101.2019.9059866.
[11] N. Raab, et al., Status of the laboratory infrastructure for detector calibration and characterization at the European XFEL, Dec, J. Instrum. 11 (2016), https://doi.org/10.1088/1748-0221/12/04/E04002, 10.1088/1748-0221/11/12/C12051 and J. Instrum., vol. 12, Apr. 2017.
[12] M. Ghisetti, et al., Impact of X-ray spectra modeling on gain and noise determination in high-dynamic range detection systems, in: 2022 IEEE Nuclear Science Symposium and Medical Imaging Conference, NSS/MIC), Milano, Italy, 2022, pp. 1–3.
[13] S. Schlee, et al., Methods for calibrating the gain and offset of the DSSC detector for the European XFEL using X-ray line sources, J. Instrum. 11 (1) (2016), https://doi.org/10.1088/1748-0221/11/01/C01001.
[14] G. Phillips, K. Marlow, Automatic analysis of gamma-ray spectra from germanium detectors, Nucl. Instrum. Methods 137 (1976) 525.